The Astrophysical Journal Letters, 792:L39 (6pp), 2014 September 10 doi:10.1088/2041-8205/792/2/L39
© 2014. The American Astronomical Society. All rights reserved. Printed in the U.S.A.

THE DROP DURING LESS THAN 300 DAYS OF A DUSTY WHITE DWARF'S INFRARED LUMINOSITY

S. Xu (许偲艺) and M. Jura
Department of Physics and Astronomy, University of California, Los Angeles, CA 90095-1562, USA; sxu@astro.ucla.edu, jura@astro.ucla.edu
Received 2014 June 12; accepted 2014 August 2; published 2014 August 28

ABSTRACT

We report *Spitzer*/Infrared Array Camera photometry of WD J0959−0200, a white dwarf that displays excess infrared radiation from a disk, likely produced by a tidally disrupted planetesimal. We find that in 2010, the fluxes in both 3.6 μm and 4.5 μm decreased by ∼35% in less than 300 days. The drop in the infrared luminosity is likely due to an increase of the inner disk radius from one of two scenarios: (1) a recent planetesimal impact; (2) instability in the circumstellar disk. The current situation is tantalizing; high-sensitivity, high-cadence infrared studies will be a new tool to study the interplay between a disk and its host white dwarf star.

Key words: circumstellar matter – minor planets, asteroids: general – white dwarfs

Online-only material: color figures

1. INTRODUCTION

The discovery of an infrared excess around a single white dwarf G29-38 (Zuckerman & Becklin 1987) from an orbiting dust disk (Graham et al. 1990) helped lay the foundation for the study of planetary systems around white dwarfs. However, it was not until much later that a now widely accepted model was proposed to explain the source of the dust—tidal disruption of planetesimals (Debes & Sigurdsson 2002; Jura 2003). Subsequent progress has been rapid, particularly after the discovery of an infrared excess around a second white dwarf GD 362 (Kilic et al. 2005; Becklin et al. 2005). Various dynamical pathways have been explored to deliver the planetesimals into the white dwarf tidal radius (Bonsor et al. 2011; Veras et al. 2013; Frewen & Hansen 2014; Mustill et al. 2014). Eventually, all these materials get accreted onto the white dwarf and enrich its pure hydrogen or/and helium atmosphere. Studying these heavy-element-enriched white dwarfs has become a uniquely powerful way to directly measure the bulk compositions of extrasolar planetesimals (von Hippel et al. 2007; Zuckerman et al. 2007; Klein et al. 2010; Farihi et al. 2010; Gänsicke et al. 2012; Jura et al. 2012; Xu et al. 2014; Jura & Young 2014).

To date, mainly due to the launch of the *Spitzer Space Telescope*, more than 30 dusty white dwarfs have been identified (Farihi et al. 2009; Debes et al. 2011; Xu & Jura 2012; Barber et al. 2014). The spectral energy distributions (SEDs) can be fit with a geometrically thin, optically thick disk within the tidal radius of the white dwarf (Jura 2003). The typical disk lifetime is estimated to be 10^5–10^6 yr (Jura 2008; Rafikov 2011a, 2011b; Girven et al. 2012). The disk occurrence rate is about 4% for white dwarfs between 9500 and 22,500 K (Barber et al. 2012). Despite intensive searches, only one disk host star G166-58 has an effective temperature less than 9500 K (Farihi et al. 2008; Xu & Jura 2012). When observed with a high-resolution optical/ultraviolet spectrograph, all dusty white dwarfs show a high level of atmospheric enrichment of heavy elements.[1] Circumstellar gaseous material has also been detected around some white dwarfs (Gänsicke et al. 2006; Melis et al. 2010; Brinkworth et al. 2012; Debes et al. 2012).

There are many puzzles regarding these dusty white dwarfs. How massive is the dust disk? How does the disk evolve with time? Why do some of them show calcium triplet emission lines from the circumstellar gas while others do not? In addition, these emission lines appear to be variable on timescale of a few years (Gänsicke et al. 2008). What causes such variability?

In this Letter, we report the first result from a systematic study of infrared variability for dusty white dwarfs. We focus on one target, WD J0959−0200, whose fluxes have decreased by ∼35% in the infrared.

2. OBSERVATIONS AND DATA REDUCTION

2.1. Source Selection

Most dusty white dwarfs have been observed with the Infrared Array Camera (IRAC; Fazio et al. 2004) at 3–10 μm, where the disk emits most of its flux. When the *WISE* data became available, we compared the fluxes of all dusty white dwarfs at W-1 with IRAC-1 and W-2 with IRAC-2. We found that the flux level was comparable for the majority of them, but a few showed disparities larger than 3σ; most of them have a larger *WISE* fluxes due to the lower spatial resolution of *WISE* and contamination from background sources (also see Figure 1). In particular, five white dwarfs were in a clean field with no obvious contaminating source in the IRAC image and this discrepancy can be real. We were awarded *Spitzer* time in cycle 10 to re-investigate these five targets. The program is still ongoing and we report the result of WD J0959−0200 in this Letter.

WD J0959−0200 is a hydrogen-dominated white dwarf discovered by the Sloan Digital Sky Survey (SDSS) with a *K*-band excess from the United Kingdom Infrared Telescope (UKIRT) Infrared Deep Sky Survey (UKIDSS; Girven et al. 2011). Follow-up observation from *Spitzer* shows that this star indeed has an infrared excess from an orbiting dust disk. Spectroscopic observations with the Very Large Telescope (VLT) show photospheric absorption lines from calcium, magnesium, as well as infrared calcium triplet emission (Farihi et al. 2012a). With a stellar temperature of 13,280 K, WD J0959−0200 is the coolest dusty white dwarf with circumstellar gaseous material, whose effective temperatures range between 13,280 K and 20,700 K.

[1] With the *Wide-field Infrared Survey Explorer* (*WISE*), Hoard et al. (2013) identified three potential dusty white dwarfs with no heavy elements in their atmospheres. However, they also noted that they are only candidates for having a dust disk due to possible background contamination.

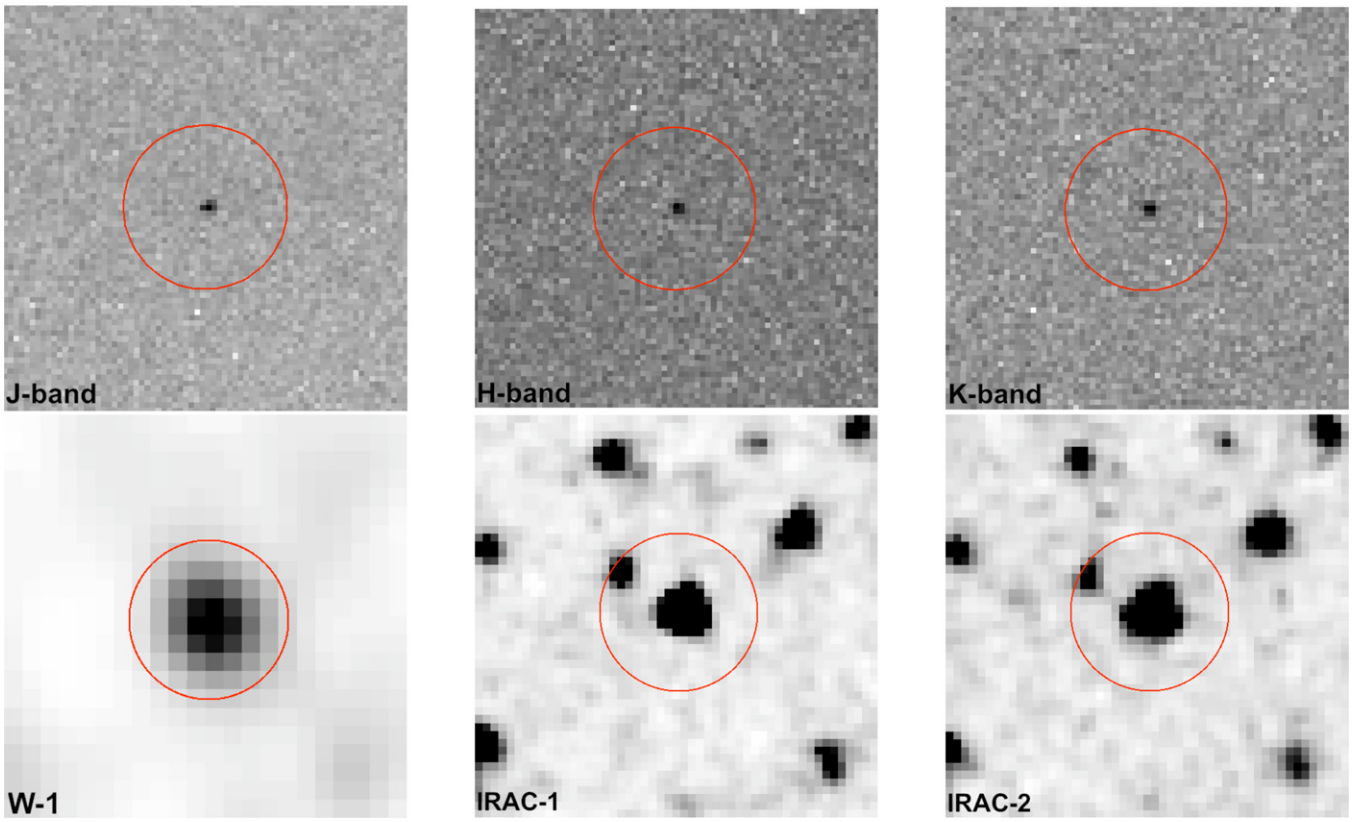

Figure 1. Images for WD J0959−0200 in the *J*, *H*, and *K* bands (UKIRT, 2014 March), W-1 band from ALLWISE, as well as *Spitzer*/IRAC bands (2014 February). North is up and east is left. The field of view is 30.″0 by 30.″0. The red circles are centered on WD J0959−0200 with a radius of 6.″0, the resolution of *WISE*. In the IRAC images, there is a background source 5.″7 away from the target, which can affect the *WISE* results. The IRAC images are much deeper than the *WISE* image due to its higher sensitivity and longer exposure times.

(A color version of this figure is available in the online journal.)

Table 1
Multiwavelength Photometry for WD J0959−0200

UT Date	Instrument	Flux (μJy)			Ref
2005 Dec 28	WFCAM	J: 72 ± 4	H: 55 ± 5	K: 57 ± 6	(1)
2014 Mar 27	WFCAM	J: 73 ± 3	H: 54 ± 4	K: 46 ± 3	(2)
2010 Jan 06	IRAC[b]	IRAC-1: 80 ± 4	IRAC-2: 76 ± 4		(3)
2010 May 18 & Nov 24[a]	*WISE*[b]	W-1: 46 ± 6[c]	W-2: 41 ± 10[c]		(4)
2014 Feb 04	IRAC[b]	IRAC-1: 52 ± 3	IRAC-2: 50 ± 3		(2)

Notes.
[a] WD J0959−0200 was observed by *WISE* at two different epochs but the intrinsic faintness of this star does not allow for reliable photometric measurement at each epoch.
[b] Central wavelengths for IRAC bands are 3.6 μm and 4.5 μm; for *WISE* bands, they are 3.4 μm and 4.5 μm.
[c] This is the corrected flux by subtracting the flux of the background source measured from IRAC, see Section 2.4 for details.
References. (1) UKIDSS; (2) measurement from this Letter; (3) Farihi et al. (2012a), our measurement also agrees with their values; (4) ALLWISE.

In comparison, dusty white dwarfs typically have a temperature range of 9500–23,100 K (Brinkworth et al. 2012).

Because a large portion of the *K*-band flux for WD J0959−0200 is also from the dust disk, we obtained additional *JHK* photometry with UKIRT. The observing logs are presented in Table 1.

2.2. *Spitzer*

WD J0959−0200 was observed with IRAC on warm *Spitzer* (Werner et al. 2004) in 2010 (PI: J. Farihi). The observing strategy and data analysis were described in Farihi et al. (2012a). We reobserved this target in 2014 (PI: M. Jura) with a similar configuration—30 s exposure with 30 medium-size dithers in the cycling pattern, resulting in a total of 900 s on target time in each channel.

Following data reduction procedures outlined in Farihi et al. (2010) and Xu & Jura (2012), we used MOPEX to create the final mosaic of 0.″6 pixel^{-1}, as shown in Figure 1. In the IRAC bands, WD J0959−0200 is well separated from all nearby sources. However, there is a background source 5.″7 away, which could affect the *WISE* results (see Section 2.4). We performed aperture photometry with PHOT in IRAF and the results are presented in Table 1.

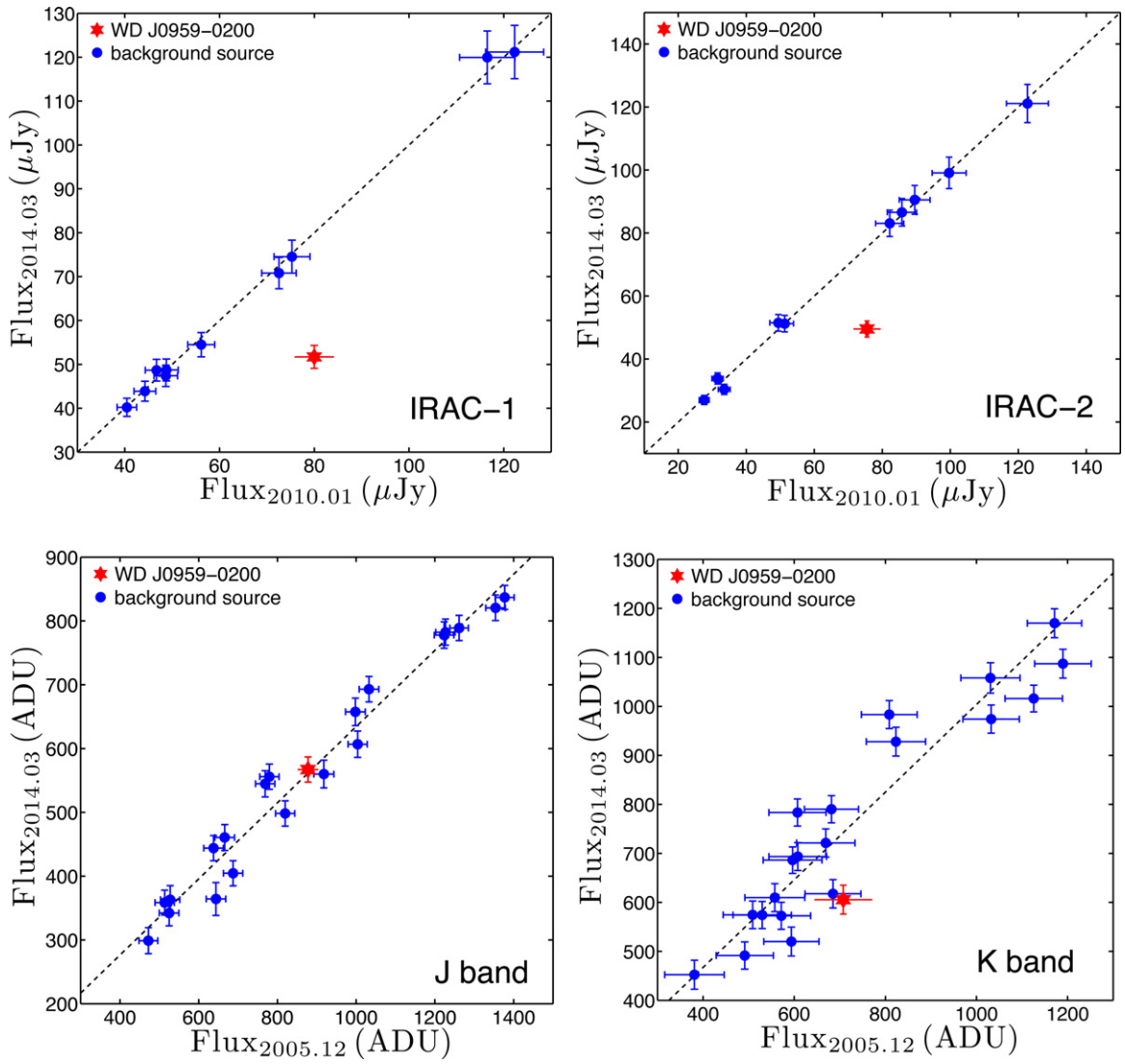

Figure 2. Photometric measurements for WD J0959−0200 and nearby sources at different observing times, indicated by the subscripts. Upper panels: *Spitzer*/IRAC data. The dashed lines represent 1:1 correlations. The fluxes for WD J0959−0200 have decreased significantly in both IRAC bands. Lower panels: *J*- and *K*-band data from the UKIRT. The black dashed lines represent the least squares fit to the 20 nearby sources. The *J*-band flux has stayed the same while likely the *K*-band flux has decreased, consistent with the IRAC results.

(A color version of this figure is available in the online journal.)

Relative to the 2010 data, we find that the flux for WD J0959−0200 decreased 35% ± 4% and 34% ± 4% in IRAC-1 and IRAC-2, respectively. As a sanity check, we also measured the fluxes of 10 nearby stars that have comparable fluxes and are in a clean field. As shown in Figure 2, the standard deviation between the two epochs for the comparison targets is 1.3% in IRAC-1 and 2.0% in IRAC-2, much smaller than the observed flux differences for WD J0959−0200. The decrease of flux for WD J0959−0200 is real.

2.3. UKIRT

WD J0959−0200 was observed in 2005 with the Wide Field Camera (WFCAM) as part of the Large Area Survey (LAS) in the UKIDSS (Lawrence et al. 2007). Four broadband photometric observations at *Y*, *J*, *H*, and *K* with an exposure time of 40 s each were obtained.

In 2014, we were awarded UKIRT DDT time to reobserve WD J0959−0200. A number of exposures were taken with 10 s each. The total on target time was 150 s, 450 s, and 1250 s for the *J*, *H*, and *K* bands, respectively. No flux standard was taken. The raw data were processed by the pipeline from the Cambridge Astronomical Survey Unit (CASU) and individual frames were combined in IRAF to produce the final mosaic, as shown in Figure 1. We performed aperture photometry on the target as well as a few nearby sources. Because UKIDSS data covered the same surrounding stars, we used their published magnitudes to derive the flux calibration of the 2014 UKIRT data. The photometry results for WD J0959-0200 are listed in Table 1 and we see its *K*-band flux might have decreased.

To further investigate the flux level for WD J0959−0200 in the two epochs, we performed aperture photometry on both the UKIDSS data and the 2014 UKIRT data. The flux unit was kept in analog to digital unit (ADU), which is directly from the raw data. This avoids introducing additional uncertainties from flux calibration because these stars are close to the limiting magnitude of the UKIDSS survey. A least squares fit on the 20 nearby sources is used to find the conversion between the two epochs, as shown in Figure 2. Relative to the flux in 2005, the *J*-, *H*-, and *K*-band fluxes for WD J0959−0200 in 2014 are 101.0% ± 4.5%, 99.1% ± 10.8% and 81.5% ± 8.1%,

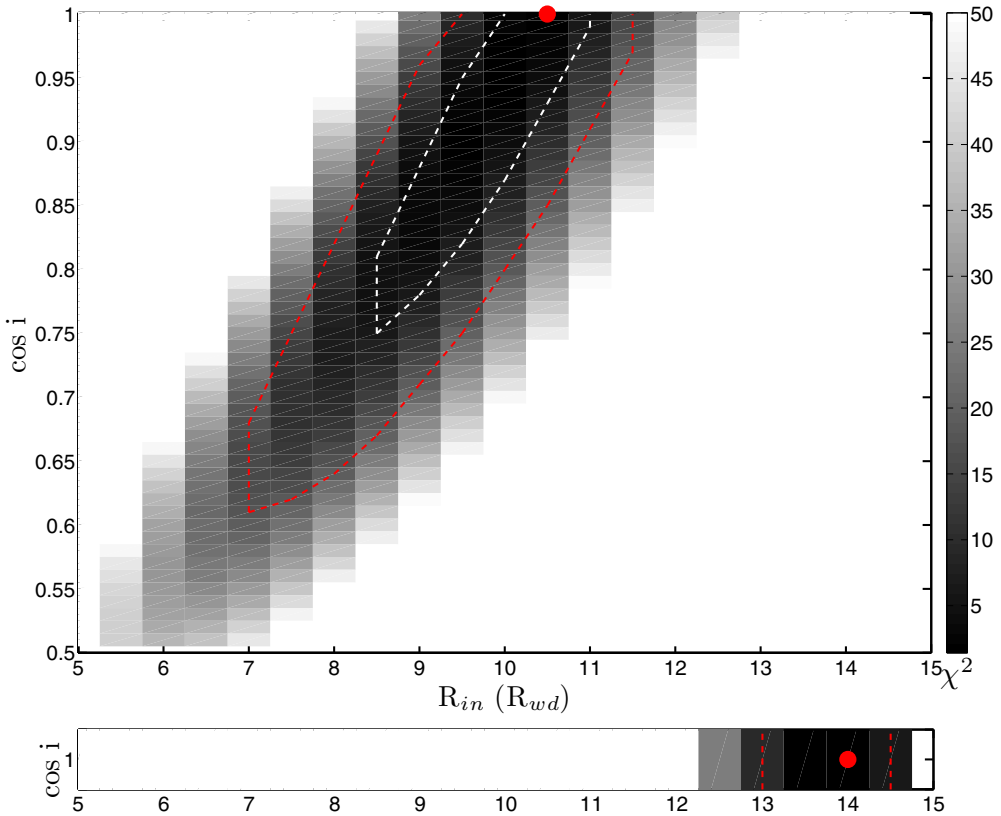

Figure 3. Least χ^2 fitting for the SED of WD J0959-0200. Top panel: a slice of the χ^2 volume for pre-March 2010 data with $R_{\rm out} = 26.5\ R_{\rm wd}$. The red dot is the least χ^2 value of 1.42. The white dashed line is the 1σ contour, which represents a disk inclination between 0 deg and 41 deg and an inner radius, $R_{\rm in}$, between 8.5 $R_{\rm wd}$ and 11 $R_{\rm wd}$; the red dashed line is the 3σ contour that has a disk inclination between 0 deg and 52 deg and $R_{\rm in}$ between 7 $R_{\rm wd}$ and 11.5 $R_{\rm wd}$. A nearly face-on disk with a small inner radius is required to fit the SED. Bottom panel: χ^2 fitting for the post-March 2010 data with $R_{\rm out} = 26.5\ R_{\rm wd}$ and $\cos\ i = 1$. The red dot is the least χ^2 value of 11.5. The red dashed line represents the 3σ boundary and has $R_{\rm in}$ between 13.0 $R_{\rm wd}$ and 14.5 $R_{\rm wd}$.

(A color version of this figure is available in the online journal.)

respectively. It is likely that the *K*-band flux for WD J0959−0200 has decreased, consistent with the *Spitzer* results.

2.4. *WISE*

The ALLWISE fluxes are $55 \pm 6\ \mu$Jy for W1 and $49 \pm 10\ \mu$Jy for W2. In addition, the IRAC images show that there is a background source within the *WISE* resolution of 6.″0 (see Figure 1) and the measured fluxes are $9 \pm 2\ \mu$Jy and $8 \pm 2\ \mu$Jy for IRAC-1 and IRAC-2, respectively. We subtract those numbers from the ALLWISE data and list the corrected *WISE* fluxes in Table 1.

3. DISCUSSION

The most stringent constraint on the duration of the infrared variability is between the first IRAC and *WISE* observations, which are 4–10 months apart. Luckily, optical spectroscopic observations with the VLT/X-Shooter of WD J0959−0200 were obtained in 2010 June and 2011 March, around the same time that *WISE* data were taken. No variations in the photospheric absorption lines or calcium triplet emission lines were reported. Given that WD J0959−0200 is directly accreting from the disk and the settling times of heavy elements are only days, there must have been little change in the physical conditions between the two epochs. It is likely that the drop in the infrared luminosity has taken place in less than five months, between the first IRAC observation in 2010 January and the first X-Shooter observation in 2010 June. However, it is more conservative to estimate a duration of the drop to be less than 10 months given the uncertainties in the individual measurements. The actual duration can be much shorter.

3.1. SED Fits

The white dwarf spectrum is calculated using TLUSTY and SYNSPEC (Hubeny & Lanz 1995) and input parameters of $T_{\rm wd} = 13{,}280$ K and $\log g = 8.06$ (Farihi et al. 2012a). To fit the SED of the dust disk, we use the opaque disk model described in Jura (2003) with three free parameters, the inner disk radius $R_{\rm in}$, outer disk radius $R_{\rm out}$, and disk inclination i. The inner and outer disk radii are most sensitive to $\sim 3\ \mu$m and $8\ \mu$m fluxes, respectively, while the disk inclination affects all the infrared flux. For the majority of dusty white dwarfs, the inner disk radius corresponds to a disk temperature of 1200 K, the characteristic sublimation temperature for silicates. The outer disk radius varies but is always within the tidal radius of the white dwarf.

For the pre-March 2010 data, we find the fractional luminosity $L_{\rm IR}/L_{\rm wd} = 0.03$, the highest of all dusty white dwarfs (Farihi et al. 2010). A face-on disk with a small inner disk radius, correspondingly a high inner disk temperature, is needed to fit the SED. The best-fit disk parameters are $R_{\rm in} = 10.5 R_{\rm wd}$ ($T_{\rm in} =$ 1545 K), $R_{\rm out} = 26.5\ R_{\rm wd}$ ($T_{\rm out} = 771$ K), $i = 0°$, and $\chi^2 =$ 1.42 with five degrees of freedom from the fluxes of the *JHK* bands and the IRAC bands. The outer disk radius is not as well constrained due to the lack of data from longer wavelengths. A slice of the χ^2 volume is shown in Figure 3. A less face-on disk with an even smaller inner radius can also fit the data; however,

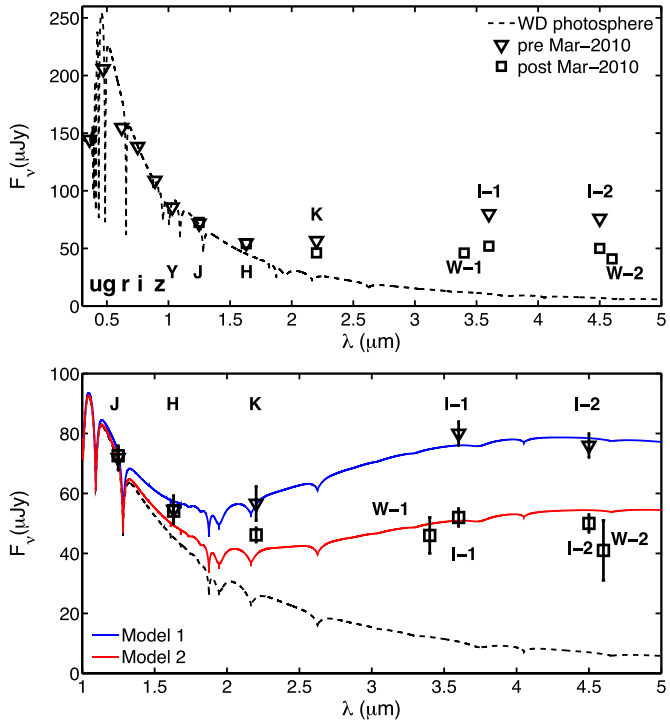

Figure 4. SED fits for WD J0959−0200 with photometric data from the SDSS (*ugriz*), UKIRT (*YJHK*), *WISE* (W-1, W-2 = bands 1 and 2, respectively), and *Spitzer*/IRAC (I-1, I-2 = bands 1 and 2, respectively). The upper panel shows the entire SED and the lower panel shows only the infrared part. The black dashed line is the simulated spectrum for WD J0959−0200. The blue and red solid lines represent models that fit the pre-March 2010 and post-March 2010 data, respectively. The only difference between these two models is the inner disk radius, which has increased from 10.5 $R_{\rm wd}$ in Model 1 to 14 $R_{\rm wd}$ in Model 2.

(A color version of this figure is available in the online journal.)

it would require a even higher inner disk temperature, which is more difficult to achieve. The SED with the best fit model is shown in Figure 4. A caveat here is that there are four years between the UKIDSS and IRAC data and there could have been additional changes in the disk. However, the high fractional luminosity of the disk makes the quality of the fit insensitive to the likely range of the *K*-band magnitude.

For the post-March 2010 data, the fractional luminosity has dropped to 0.02, which is still on the high side for dusty white dwarfs. There is no unique fit to the near infrared data due to the degeneracy between the inner disk radius and disk inclination. Fortunately, we can use the calcium triplet lines, which are much weaker and narrower than the other known cases; Farihi et al. (2012a) derived a nearly face-on disk with an inclination of 11°. We set $R_{\rm out} = 26.5\,R_{\rm wd}$, $i = 0°$—the same as the model for pre-March 2010 data—and find the best fit model requires $R_{\rm in} = 14\,R_{\rm wd}$ ($T_{\rm in} = 1245$ K). The χ^2 fitting is shown in Figure 3 and the SED is shown in Figure 4. Even though the computed SED underestimates the *K*-band flux, the model has a χ^2 value of 11.5, which is within 3σ. With all the available data, an increase of the inner disk radius from $10.5^{+1.0}_{-3.5}$ $R_{\rm wd}$ to $14.0^{+0.5}_{-1.0}$ $R_{\rm wd}$ is the most plausible explanation for the drop of the infrared luminosity of WD J0959−0200.

3.2. Interpretations

What can cause such a change in the inner disk radius? We explore two scenarios and propose some experiments to test these hypotheses.

A recent planetesimal impact. Wyatt et al. (2014) suggest that the tidal disruption of small planetesimals around white dwarfs can be nearly continuous. It is unlikely that the newcoming asteroid has the exact same orbital inclination as the pre-existing dust disk. Jura (2008) showed that during an impact, the dust disk will be eroded by sputtering and the infrared flux will decrease within 600 yr, possibly much shorter. To increase the inner radius from 10.5 $R_{\rm wd}$ to 14 $R_{\rm wd}$, the disk has decreased 5×10^{10} km^2 in surface area, much larger than the typical size of an asteroid in the solar system. For comparison, there exist dusty white dwarfs with much larger inner holes, e.g., PG 1225-079 and G166-58, possibly also due to planetesimal impacts (Farihi et al. 2010). Recently, the tidal disruption of an entire planet by a white dwarf has been invoked to explain the light curve of a source in the center of a globular cluster (Del Santo et al. 2014).

Instability in the circumstellar disk. WD J0959−0200 belongs to the rare category of dusty white dwarfs that also display calcium triplet emission lines from an orbiting gaseous disk (Farihi et al. 2012a). To fit the pre-March 2010 SED, even with a face-on disk, a high inner disk temperature of 1545 K is required, much higher than the characteristic temperature for rapid silicate sublimation.[2] Rafikov & Garmilla (2012) and Metzger et al. (2012) found that this super-heated inner disk region is unstable and interactions between the dust and gaseous material can cause rapid changes in the physical conditions. This can lead to a change in the viscosity of the gas and accretion rate onto the white dwarf. A flare is expected to occur (Bear & Soker 2013), similar to what happens during dwarf novae outbursts (e.g., Lasota 2001). To estimate the total mass loss, we approximate the average mass of heavy elements in a dusty helium white dwarfs' atmosphere 10^{22} g as the disk mass. Increasing the inner disk radius from 10.5 $R_{\rm wd}$ to 14 $R_{\rm wd}$ corresponds to a total mass loss of 3.3×10^{20} g. The derived mass accretion rate is at least $\sim 1.3 \times 10^{13}$ g s^{-1} and an accretion luminosity of 1.5×10^{30} erg s^{-1}, which is nearly 10% of the bolometric luminosity of WD J0959−0200. Much of the accretion luminosity is likely to be emitted as X-rays (Jura et al. 2009), that might be detectable with current X-ray facilities. In addition, there can also be optical transient events associated with the accretion, as seen in dwarf novae (Bear & Soker 2013).

We estimate that ∼3% of the mass of the disk was accreted onto the white dwarf in less than 300 days, while the disk lifetime is estimated to be 10^5–10^6 yr. One possible implication is that the accretion occurs in short, intense bursts rather than in a steady state, as argued by Farihi et al. (2012b). Future high-precision, high-cadence infrared photometric observations will be essential to disentangle different scenarios. If we can measure the photospheric abundance when the infrared flux is changing, we may have the opportunity to witness the specific composition of an incoming planetesimal. That is, the settling times of heavy elements can be quite short, e.g., a few days in WD J0959−0200, and we can imagine the observed abundance to change on a similarly short timescale.

4. CONCLUSIONS

We report the drop of infrared luminosity of a dusty white dwarf, WD J0959−0200, in less than 300 days in 2010; the actual duration might be even shorter. Such a change can be caused by an increase in the inner disk radius. We provide two

[2] The majority of gas disk host white dwarfs require a similar high inner disk temperature (Brinkworth et al. 2012). The cause is unknown.

hypotheses to explain the change, a recent planetesimal impact and instability in the circumstellar disk. Future observations in the time domain would greatly improve our knowledge of the fate of planetary systems around white dwarfs.

The authors thank an anonymous referee for helpful comments. S. Xu thanks R. Mostardi for helpful discussions on data reduction with IRAF. This work has been supported by the NSF. It is based in part on observations made with (1) the *Spitzer Space Telescope*, which is operated by JPL, Caltech under a contract with NASA; (2) *WISE*, which is a joint project of UCLA and JPL/Caltech, funded by NASA; (3) data obtained as part of the UKIDSS. We also thank Richard Green for awarding us DDT time on the UKIRT and Tom Kerr for carrying out the observation.

REFERENCES

Barber, S. D., Kilic, M., Brown, W. R., & Gianninas, A. 2014, ApJ, 786, 77
Barber, S. D., Patterson, A. J., Kilic, M., et al. 2012, ApJ, 760, 26
Bear, E., & Soker, N. 2013, NewA, 19, 56
Becklin, E. E., Farihi, J., Jura, M., et al. 2005, ApJL, 632, L119
Bonsor, A., Mustill, A. J., & Wyatt, M. C. 2011, MNRAS, 414, 930
Brinkworth, C. S., Gänsicke, B. T., Girven, J. M., et al. 2012, ApJ, 750, 86
Debes, J. H., Hoard, D. W., Wachter, S., Leisawitz, D. T., & Cohen, M. 2011, ApJS, 197, 38
Debes, J. H., Kilic, M., Faedi, F., et al. 2012, ApJ, 754, 59
Debes, J. H., & Sigurdsson, S. 2002, ApJ, 572, 556
Del Santo, M., Nucita, A. A., Lodato, G., et al. 2014, arXiv:1407.5081
Farihi, J., Gänsicke, B. T., Steele, P. R., et al. 2012a, MNRAS, 421, 1635
Farihi, J., Gänsicke, B. T., Wyatt, M. C., et al. 2012b, MNRAS, 424, 464
Farihi, J., Jura, M., Lee, J.-E., & Zuckerman, B. 2010, ApJ, 714, 1386
Farihi, J., Jura, M., & Zuckerman, B. 2009, ApJ, 694, 805
Farihi, J., Zuckerman, B., & Becklin, E. E. 2008, ApJ, 674, 431
Fazio, G. G., Hora, J. L., Allen, L. E., et al. 2004, ApJS, 154, 10
Frewen, S. F. N., & Hansen, B. M. S. 2014, MNRAS, 439, 2442
Gänsicke, B. T., Koester, D., Farihi, J., et al. 2012, MNRAS, 424, 333
Gänsicke, B. T., Koester, D., Marsh, T. R., Rebassa-Mansergas, A., & Southworth, J. 2008, MNRAS, 391, L103
Gänsicke, B. T., Marsh, T. R., Southworth, J., & Rebassa-Mansergas, A. 2006, Sci, 314, 1908
Girven, J., Brinkworth, C. S., Farihi, J., et al. 2012, ApJ, 749, 154
Girven, J., Gänsicke, B. T., Steeghs, D., & Koester, D. 2011, MNRAS, 417, 1210
Graham, J. R., Matthews, K., Neugebauer, G., & Soifer, B. T. 1990, ApJ, 357, 216
Hoard, D. W., Debes, J. H., Wachter, S., Leisawitz, D. T., & Cohen, M. 2013, ApJ, 770, 21
Hubeny, I., & Lanz, T. 1995, ApJ, 439, 875
Jura, M. 2003, ApJL, 584, L91
Jura, M. 2008, AJ, 135, 1785
Jura, M., Muno, M. P., Farihi, J., & Zuckerman, B. 2009, ApJ, 699, 1473
Jura, M., Xu, S., Klein, B., Koester, D., & Zuckerman, B. 2012, ApJ, 750, 69
Jura, M., & Young, E. D. 2014, AREPS, 42, 45
Kilic, M., von Hippel, T., Leggett, S. K., & Winget, D. E. 2005, ApJL, 632, L115
Klein, B., Jura, M., Koester, D., Zuckerman, B., & Melis, C. 2010, ApJ, 709, 950
Lasota, J.-P. 2001, NewAR, 45, 449
Lawrence, A., Warren, S. J., Almaini, O., et al. 2007, MNRAS, 379, 1599
Melis, C., Jura, M., Albert, L., Klein, B., & Zuckerman, B. 2010, ApJ, 722, 1078
Metzger, B. D., Rafikov, R. R., & Bochkarev, K. V. 2012, MNRAS, 423, 505
Mustill, A. J., Veras, D., & Villaver, E. 2014, MNRAS, 437, 1404
Rafikov, R. R. 2011a, ApJL, 732, L3
Rafikov, R. R. 2011b, MNRAS, 416, L55
Rafikov, R. R., & Garmilla, J. A. 2012, ApJ, 760, 123
Veras, D., Mustill, A. J., Bonsor, A., & Wyatt, M. C. 2013, MNRAS, 431, 1686
von Hippel, T., Kuchner, M. J., Kilic, M., Mullally, F., & Reach, W. T. 2007, ApJ, 662, 544
Werner, M. W., Roellig, T. L., Low, F. J., et al. 2004, ApJS, 154, 1
Wyatt, M. C., Farihi, J., Pringle, J. E., & Bonsor, A. 2014, MNRAS, 439, 3371
Xu, S., & Jura, M. 2012, ApJ, 745, 88
Xu, S., Jura, M., Koester, D., Klein, B., & Zuckerman, B. 2014, ApJ, 783, 79
Zuckerman, B., & Becklin, E. E. 1987, Natur, 330, 138
Zuckerman, B., Koester, D., Melis, C., Hansen, B. M., & Jura, M. 2007, ApJ, 671, 872